# Layer by Layer Immobilized Horseradish Peroxidase on Zinc Oxide Nanorods for Biosensing

**B. X. Gu, C. X. Xu,* and G. P. Zhu**

*Advanced Photonics Centre, School of Electronic Science and Engineering Southeast University, Nanjing 210096, P. R. China*

**S. Q. Liu,* L. Y. Chen, and M. L. Wang**

*School of Chemistry and Chemical Engineering, Southeast University, Nanjing 211189, P. R. China*

**J. J. Zhu**

*Laboratory of Life Analytical Chemistry, School of Chemistry and Chemical Engineering, Nanjing University, Nanjing 210093, P. R. China*

*Received: January 3, 2009; Revised Manuscript Received: March 19, 2009*

Using zinc powders as source material, ZnO nanorods (ZnONR) were fabricated on gold wire by a hydrothermal reaction without any other surfactant. The gold wire end was coated by a thin layer of Zn−Au alloy to improve the nucleation for growth of ZnO nanostructures and to further improve the performance of the biosensor, which was constructed by alternatively immobilizing poly(sodium 4-styrenesulfonate) (PSS) and horseradish peroxidase (HRP) on the ZnONR. Electrochemical measurement, ultraviolet−visible spectrum, $\zeta$-potential, and scanning electron microscopic analysis demonstrated that PSS and HRP were stably adsorbed layer by layer on the ZnONR surface, and the HRP kept bioactivity for $H_2O_2$ detection without an electron transfer mediator. The multilayered HRP sensors exhibited a wide linear range and low detection limit. The sensitivity of the biosensor increased with the immobilized HRP layers from the lowest value of 36.28 $\mu$A $mM^{-1}$ for a monolayer.

## 1. Introduction

In recent years, nanostructural ZnO has attracted considerable interest due to its wide direct band gap, strong exciton binding energy, aesthetic morphologies, and multifunctional applications. Besides the optoelectronic properties, nanostructural ZnO also possesses many advantages for biosensoring, such as high aspect ratio, polar surface along the *c*-axis, good electron communication, nontoxic and safe for living organisms. In particular, the isoelectric point (IEP) of ZnO is as high as about 9.5, which is suitable for immobilization of molecules with low IEP, such as poly(sodium 4-styrensulfonate) (PSS) and some proteins, assisted by electrostatic attraction in proper pH value.[1] So far, ZnO nanoparticles, porous films, nanocombs, and nanorods have been developed into biosensors to detect cytochrome *c*,[1−3] protein,[4] uric acid,[5] glucose,[6,7] and phenolic compounds,[8] respectively.

Horseradish peroxidase (HRP) is an important enzyme consisting of a heme catalytic center and the surrounding protein. The heme group contains an Fe(III)/Fe(II) redox couple. Since the direct electron transfer of HRP adsorbed on a carbon electrode was first reported by Yaropolov et al.[9] in 1978, various materials such as $TiO_2$ nanotubes[10] and gold nanoparticles[11] have revealed similar function. To improve the performance of such biosensors, a multilayer biomolecular immobilization technique has been developed in recent years; for example, layer by layer modified HRP/protein has been employed to investigate the damage of protein by $H_2O_2$.[12] Especially in immunosensors, the multilayer immobilization technique has improved the detection limits for antigen or DNA as low as 7 pg/mL or 40 fM through.[13] It provides a quick and effective method for early diagnosis of disease.

In the present work, the ZnONR were hydrothermally grown directly on the gold electrode which was pretreated to coat a layer of the Zn−Au alloy in order to improve the molecular immobilization efficiency and the biosensoring stability. The electronegative polymer PSS and HRP with IEP 8.9[14] were immobilized layer by layer on ZnONR to investigate the electrochemical reaction process and the biosensoring behaviors of $H_2O_2$. We shall present the construct method of the biosensor and the improved sensing characteristics in detail.

## 2. Experimental Section

**Chemicals.** Gold wire (99.99%), zinc powders (99.95%), HRP (200−300 units $mg^{-1}$, Sigma), and PSS (MW 70000, 30% solution, Aldrich) are commercial. Before the measurements, 0.05 M phosphate buffer solution (PBS) was prepared by mixing the stock standard solutions of $Na_2HPO_4$, and the $NaH_2PO_4$ was deoxygenated by bubbling with pure nitrogen at least 30 min to obtain the PBS without oxygen (WO-PBS).

**Fabrication of the ZnONR/Au Electrode.** The hydrothermal reaction has been widely employed to fabricate nanomaterials due to its simple process, low temperature, and mass product. The hydrothermal growth of ZnO nanostructures generally involves chemical reaction between a zinc salt and an amine compound in water or water−ethanol assisted with some surficant.[15,16] Here, we just used Zn powders as the source material and a gold wire as the collection substrate to synthesize

* To whom correspondence should be addressed. E-mail: xcxseu@seu.edu.cn (C.X.X.); liusq@seu.edu.cn (S.Q.L.).

10.1021/jp900048m CCC: $40.75 
Published on Web 04/09/2009

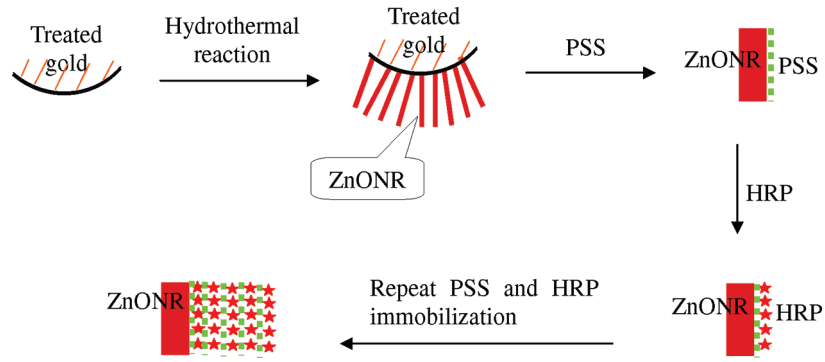


**Figure 1.** Schematic procedure of the multilayered immobilization of PSS and HRP on ZnONR.

ZnONR in deionized water. There is not any other ion or molecule in the reaction system, so the defects generated from the heterogeneous ion or molecule were avoided in the product.

Similar to our previous report,[17] the gold electrode was pretreated in order to grow ZnONR on it stably and effectively. One top of the gold wire with a 0.5 mm diameter was heated into a sphere, coated with a thin layer of zinc on the ball surface by thermal evaporation, then put into a heated tube furnace at 300 °C for 30 min to form a Zn−Au alloy layer on the gold wire, and finally immersed into boiling potassium hydroxide solution (2 M) for 2 h, and washed with deionized water.

Zinc powders (0.5 g) were put into deionized water (80 mL, >17 MΩ $cm^{-2}$) in a Teflon-inner stainless steel autoclave. The sphere end of the gold wire was vertically hung in water and sealed in the autoclave, and then, the autoclave was put into an electric oven kept at 85 °C for hydrothermal reaction to form ZnONR. After reaction for 20 h, the sample was taken out, washed with deionized water, and finally dried in air. The morphology of the product was characterized by scanning electron microscopy (SEM) (JSM-6360 LV).

**Construction of the Biosensor.** The construction procedure of the biosensor is shown in Figure 1. The ZnONR on the gold sphere were immersed into a PSS solution (1 mg $mL^{-1}$) containing 0.5 M NaCl for 0.5 h to immobilize the PSS on the ZnONR surface based on the electrostatic attraction between the positively charged ZnONR and the negatively charged PSS at pH 7.0. Then, the electrode was taken out and rinsed with deionized water to remove the free PSS. The modified PSS/ZnONR/Au was immersed into a HRP solution (2 mg $mL^{-1}$) for 5 h to immobilize the HRP on the PSS layer by attraction between the positively charged HRP and the negatively charged PSS. Then, the electrode was taken out and washed with deionized water to remove the free HRP. To improve the performance, the PSS and HRP were alternatively immobilized on ZnONR repeatedly as mentioned in the above steps. The multilayered immobilization results were examined by SEM images, ultraviolet−visible (UV−vis) absorption (Hitachi UV-3600), and ζ-potential (Zetasizer 4, Malvern Instruments).

**Electrochemical Measurements.** The electrochemical measurements were performed with a CHI 660C (CH Instrument Co. Shanghai) electrochemical workstation. In a typical three-electrode electrochemical system, the $(PSS/HRP)_n$ modified ZnONR/Au wire was employed as the working electrode, a platinum wire acted as the auxiliary electrode, and a saturated calomel electrode (SCE) acted as the reference electrode. Cyclic voltammetric (CV) and amperometric experiments were carried out in WO-PBS in a static electrochemical cell at 25 ± 0.2 °C. The solution pH value was selected as 7.0 according to the previous optimized reports[18] for HRP-catalyzed reduction of $H_2O_2$. The HRP-catalyzed electrochemical process is generally assisted by a proper electron transfer mediator to improve the detected signal.[19] In the present case, no electron transfer mediator was employed.

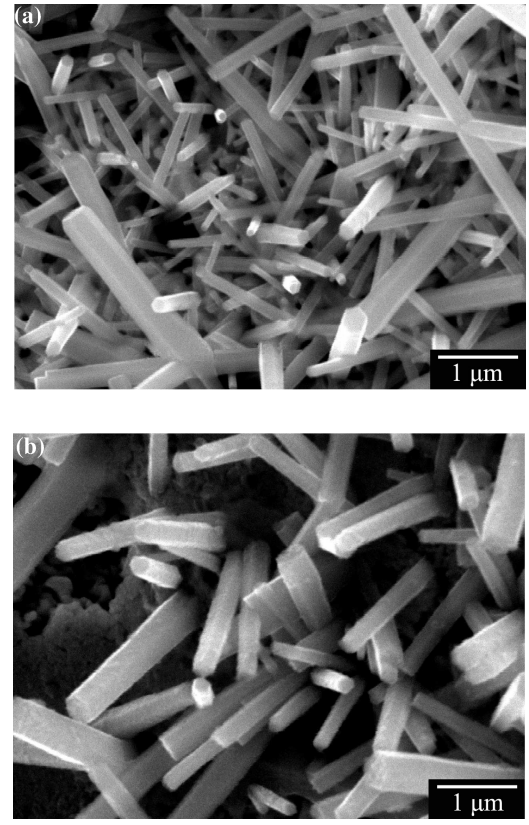


**Figure 2.** SEM images of ZnONR before (a) and after (b) immobilization of multilayer PSS/HRP.

## 3. Results and Discussion

The SEM images of the as-grown and $(PSS/HRP)_n$ modified ZnONR are shown in Figure 2. It can be seen that the smooth surface of ZnONR become rough after the multilayered immobilization. This indicated that the PSS/HRP has been modified on the ZnONR surface successfully.

The UV absorption spectra for the standard solutions of HRP (0.05 mg $mL^{-1}$) and PSS (0.125 mg $mL^{-1}$) are shown in Figure 3a. They exhibit two absorption peaks at about 410 and 275 nm from HRP[20] and another two peaks at about 258 and 224 nm from PSS. Figure 3b compares the UV absorption behaviors of the modified samples with different PSS/HRP layers on the ZnONR. Besides an invariable peak at 374 nm from the intrinsic absorption of ZnONR for all spectra, each curve hunches at about 415 nm and the inflected pitch increases with the modified

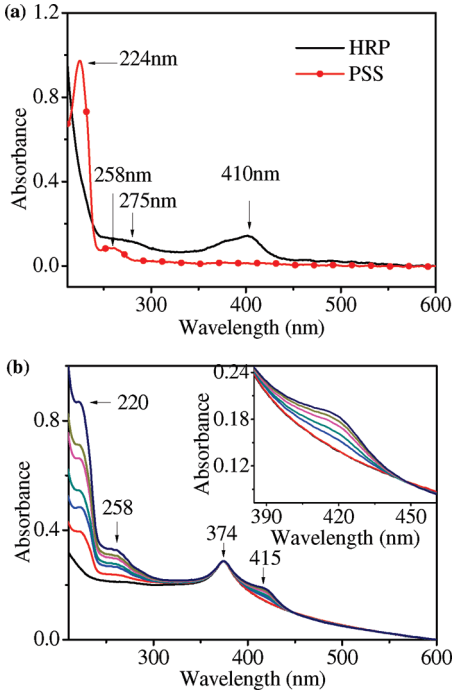


**Figure 3.** UV absorption spectra of the HRP (0.05 mg $mL^{-1}$) and PSS (0.125 mg $mL^{-1}$) standard solution (a) and layer by layer HRP/PSS modified ZnONR/Au electrode (b), inserted with the zoomed part nearby 415 nm. The curves from the bottom correspond to unmodified PSS and one- to five-layer HRP/PSS modified ZnONR/Au electrodes, respectively.

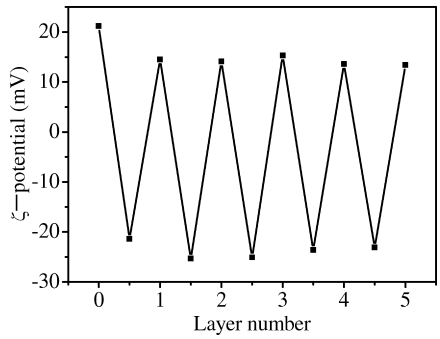


**Figure 4.** ζ-Potential variation with alternative immobilization of PSS and HRP on the of outmost layer of ZnONR.

layers, which corresponds to the HRP standard absorption at 410 nm in Figure 3a. The inset in Figure 3b presents the zoomed peaks at about 415 nm. It is clearly seen that the spectra of the naked or PSS modified ZnONR show the glossy tracks, and the absorption intensity gradually increases when the immobilized HRP is grown up from one layer to five layers. The peaks at 258 and 220 nm in Figure 3b are originated from the superposition of HRP and PSS absorption nearby these wavelengths, and the absorption intensity also increases with the HRP layers. That substantiated that the HRP and PSS were immobilized layer by layer on the ZnONR successfully.

The ζ-potential variation in Figure 4 is examined to reveal the multilayered process. As mentioned above, the ZnONR, PSS, and HRP are positively, negatively, and positively charged at pH 7.0 based on the high or low IEP values. When the negatively charged polymer PSS was immobilized on the positively charged ZnONR as the outmost layer, the negative ζ-potentials were observed. When the HRP with high IEP was immobilized on the outmost layer, the positive ζ-potentials were obtained. The alternative variation of the ζ-potentials clearly

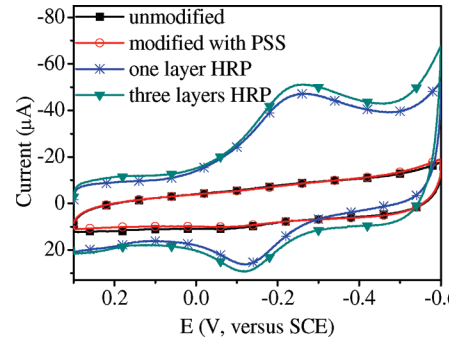


**Figure 5.** CV curves of naked, PSS modified, one- and three-layer PSS/HRP modified ZnONR/Au electrodes in pH 7.0 WO-PBS at a scan rate of 100 mV $s^{-1}$.

**TABLE 1: Key Parameters of the HRP Modified Biosensors**

| layer(s) of HRP | 1 | 2 | 3 | 4 | 5 |
|---|---|---|---|---|---|
| $10^{11} \times \Gamma^*$ (mol $cm^{-2}$) | 7.24 | 12.70 | 19.82 | 22.63 | 24.66 |
| detection limit ($\mu$M) | 2.2 | 2.4 | 1.9 | 2.5 | 2.1 |
| sensitivity ($\mu$A $mM^{-1}$) | 36.28 | 45.89 | 55.2 | 57.13 | 58.15 |
| $K_M^{app}$ ($\mu$M) | 26.13 | 23.17 | 10.72 | 12.24 | 14.57 |

revealed the effective multilayered assembly of the PSS and HRP on the ZnONR.

Figure 5 shows the CV curves of unmodified, PSS modified, monolayer, and three-layer HRP immobilized sensors in WO-PBS solution with pH 7.0. No reaction peak was observed on the curves of the naked ZnONR and the PSS modified sample. After HRP was immobilized, the direct electrochemistry of HRP on the ZnONR was obtained obviously. As shown in Figure 5, two outstanding redox peaks appear at −0.25 and −0.1 V on the curves of the electrodes immobilized with one layer and three layers of PSS/HRP, and the peak values were increasing, allowing the increase of the HRP modified layer. The cathodic and anodic peaks result from the direct electrochemistry of HRP.[21−23]

The surface concentration of electroactive HRP (Γ*) for various modified layers on electrodes were deduced from the following equation[20]

$$\Gamma^* = \frac{Q}{nFA} \quad (1)$$

where $Q$ is the charge, the electron transfer number is $n = 2$,[24] $F$ is the Faraday constant, and $A$ denotes the effective surface area of the working electrode. In order to obtain $A$, the CV experiments of naked ZnONR electrode were performed in a probe solution of 10 mM $K_3Fe(CN)_6$ at various scan rates.[25] The slope of the straight line (adjusted $r$-square = 0.9981) of $I_{pc}$ versus the square root of scan rates was $1.02 \times 10^{-4}$ A $s^{1/2}$ $V^{-1/2}$. For a reversible process,

$$I_{pc} = (2.69 \times 10^5) n^{2/3} A D^{1/2} v^{1/2} C_0 \quad (2)$$

for $K_3Fe(CN)_6$, the electron transfer number $n$ is 1, the diffusion constant $D$ is $5.9 \times 10^{-5}$ cm $s^{-2}$, $v$ is the scan rate, and $C_0$ is the concentration of solution. From eq 2, the effective surface area $A$ of the ZnONR/Au electrode can be calculated out as 0.49 $cm^2$. From the integration of the anodic peak of the sensor, the surface concentration of the active HRP on various modified layers of electrode surfaces were estimated according to eq 1 and are listed in Table 1. Following the HRP modified layer increase from one to five, the values of Γ* increased from 7.24 $\times 10^{-11}$ to 2.466 $\times 10^{-10}$ mol $cm^{-2}$. This substantiated that the amount of HRP on the ZnONR surface increased along with

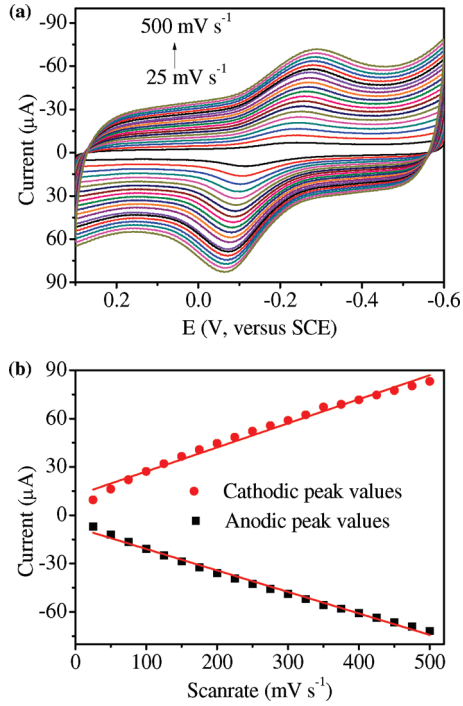


**Figure 6.** CV curve variation of a one-layer HRP modified electrode with a change of the scan rate from 25 to 500 mV with each step of 25 mV in pH 7.0 WO-PBS (a) and the plots of the cathodic and anodic peak vs the scan rate (b).

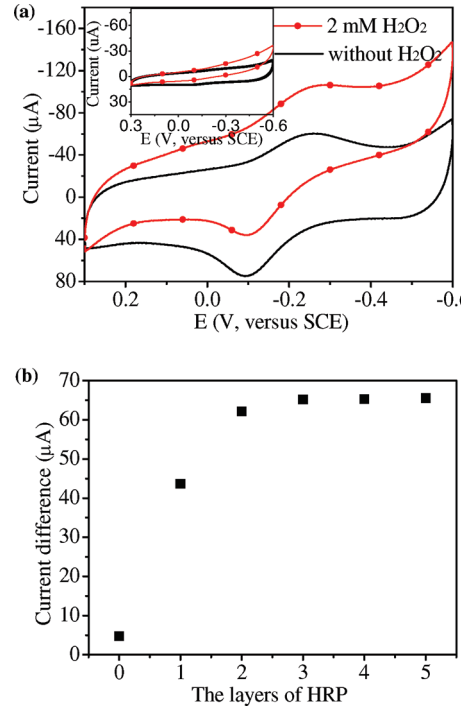


**Figure 7.** CV curves of the HRP modified electrode (a) and the difference between the cathodic peak current in the WO-PBS solution with and without 2 mM $H_2O_2$ at pH 7.0 at a scan rate of 100 mV $s^{-1}$ (b). The inset presents the CV curves of the unmodified electrode in the same solutions.

the modified-layer increase, and it is the reason that the direct electrochemistry response signal increased along with the modified-layer increase. The multilayer modified electrodes collected a higher concentration of the electroactive HRP on the surface and the monolayer HRP modified electrode presented a similar value compared with another report.[26] It substantiates that HRP was immobilized on the ZnONR layer by layer successfully.

As shown in Figure 6a, the cathodic and anodic peak current ($I_{pc}$) increased gradually when the scan rate was accelerated from 25 to 500 mV $s^{-1}$. Figure 6b plots the $I_{pc}$ versus the scan rate and reveals their linear relationship. The linear fitting to the experimental dots gives an adjusted *r*-square as high as 0.9929. This indicates that the redox reaction is a surface process and the electrons easily transfer between HRP and ZnONR/Au electrode.[25] It proved that the HRP was immobilized on the PSS/ZnONR successfully and retained its bioactivity perfectly.

The average apparent heterogeneous electron transfer rate constant $k_s$ of the immobilized HRP on the electrode surface can be estimated by the Laviron equation.[27]

$$k_s = \frac{mnFv}{RT} \tag{3}$$

where $R$ and $T$ are the gas constant and the temperature in kelvins and $m$ is correlative with the difference between the cathodic and anodic potential peak value. According to eq 3, $k_s$ is estimated as 1.15 $s^{-1}$, which is close to the reported value of some better biosensors constructed by carbon nanotubes.[28,29] It is demonstrated that the HRP immobilized on ZnONR has perfect catalysis activity, and the electrons easily transfer from HRP to electrode.

Figure 7a shows the CV curves of the electrodes with and without HRP modification in the WO-PBS solution with and without 2 mM $H_2O_2$ and their corresponding cathodic $I_{pc}$ difference in the two solutions. For the unmodified electrode, the CV curves slightly changed before and after adding 2 mM $H_2O_2$. The cathodic $I_{pc}$ of the HRP modified electrode rose obviously when the 2 mM $H_2O_2$ was added. The current increment of the HRP modified electrodes is 9 times more than that of unmodified ones. It demonstrated that the HRP immobilized on the ZnONR maintained high activity and catalyzed $H_2O_2$ reduction effectively. Figure 7b plots the cathodic $I_{pc}$ difference for naked ZnONR and HRP modified ZnONR electrodes before and after adding 2 mM $H_2O_2$. It illustrated that the cathodic $I_{pc}$ difference for ZnONR is far less than that for the HRP modified one. The cathodic $I_{pc}$ difference increased obviously when the HRP was immobilized from one layer to three layers on the ZnONR, and the difference trend to saturation over three layers. It indicated that the catalysis effect was suppressed when there were more than three HRP layers. The catalytic mechanism is exemplified as follows:[23]

$$\text{HRP (Fe}^{3+}\text{)} + \text{H}_2\text{O}_2 \rightarrow \text{compound I (Fe}^{4+}\text{=O)} + \text{H}_2\text{O} \tag{a}$$

$$\text{compound I (Fe}^{4+}\text{=O)} + \text{e} + \text{H}^+ \rightarrow \text{compound II} \tag{b}$$

$$\text{compound II} + \text{e} + \text{H}^+ \rightarrow \text{HRP (Fe}^{3+}\text{)} + \text{H}_2\text{O} \tag{c}$$

As shown in Figure 8a, the typical current−time responses of the sensors with one to five layer(s) of HRP were obtained at a working potential of −0.25 V by successively adding 5 $\mu$M (inset) and 100 $\mu$M $H_2O_2$ in pH 7.0 WO-PBS. Figure 8b shows the calibration plots of the current versus the concentration of $H_2O_2$. It demonstrates that the HRP modified biosensors exhibit a broad linear response range from 5 $\mu$M to 1.7 mM for $H_2O_2$ detection. The response time was less than 5 s when the current reached 95% of the steady-state value. The sensitivity, detection limit at a signal-to-noise ratio of 3, and apparent Michaelis−Menten constant ($K_M^{app}$) according to the Lineweaver−Burk

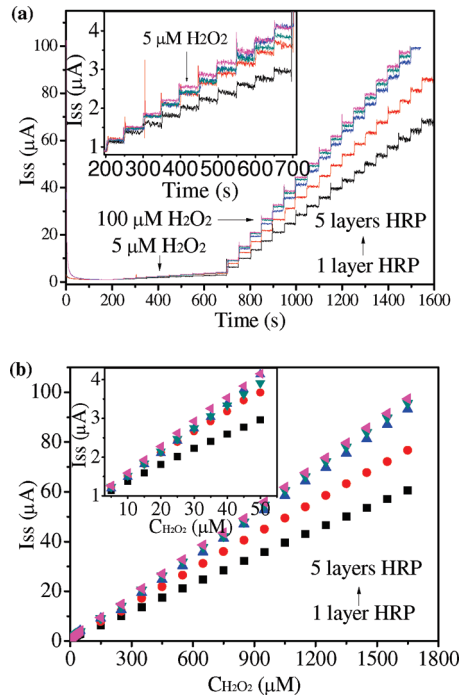


**Figure 8.** The current−time response of electrodes modified with one to five layer(s) of HRP (a) and the calibrated current−concentration relationship (b) for successively increasing $H_2O_2$ concentration in 5 $\mu$M (inset in parts a and b) and 100 $\mu$M steps at −0.25 V in pH 7.0 WO-PBS.

equation were calculated and listed in Table 1. As illustrated in Table 1, the detection limit of one to five layer(s) of HRP sensors for $H_2O_2$ detection distribute in the range 1.9−2.5 $\mu$M, which is lower than the other report.[30] The sensitivity increased from one layer to five layers of HRP. That is in accordance with the trend of Γ*. The monolayer HRP modified biosensor presents the lowest sensitivity of 36.28 $\mu$A mM$^{-1}$ which is higher than the other report.[20] The apparent $K_M^{app}$ constants are in the range of 10.72−26.3 $\mu$M, which are lower than the reported value.[30] $K_M^{app}$ decreases with the immobilized HRP layers increasing from one to three, and then increases with the further immobilization; correspondingly, the detection limit displays a similar trend. As is well-known, the lower apparent $K_M^{app}$ reflects the better affinity effect of enzyme to catalyzed target;[8,31] thus, the result demonstrates that the three-layer immobilized HRP had the maximal catalysis to $H_2O_2$ reaction.

## 4. Conclusions

In summary, a gold electrode was treated with a specific procedure that made the ZnONR grow easily and stably. The hydrothermal fabrication of ZnONR was carried out in water using Zn powders only as a source. The multilayer biomolecular immobilization technique was applied on the ZnONR/Au electrode to construct a biosensor for $H_2O_2$ detection. SEM, UV, ζ-potential, and electrochemical measurements demonstrated that the electronegative PSS and HRP with high IEP were alternately immobilized on the ZnONR successfully. The immobilized HRP on the ZnONR retained its bioactivity adequately. The multilayer biosensors exhibit a good performance. The response time is less than 5 s upon adding $H_2O_2$ to the buffer solution. $K_M^{app}$ was decreasing from 26.13 to 10.72 $\mu$M when the immobilized HRP grew from one layer to three layers, and then increased to 14.57 $\mu$M at five layers. The three-layer HRP modified sensor has the lowest $K_M^{app}$ value of 10.72 $\mu$M. Along with the immobilized HRP that grew from one layer to five layers, the Γ* was increased from 7.24 × 10$^{-11}$ to 2.466 × 10$^{-11}$ mol cm$^{-2}$, and the sensitivity was increased from 36.28 to 58.15 $\mu$A mM$^{-1}$. It is demonstrated that multilayer HRP was successfully immobilized on the ZnONR/Au electrode, and kept the bioactivity preferably for efficient catalysis to $H_2O_2$.

**Acknowledgment.** This work was supported by 863 program (2006AA03Z313), NSFC (10674023, 60725413, and 20675013), 973 program (2007CB936300), MOE key project (309015), and the NSFJ (BK2006090).

## References and Notes

(1) Topoglidis, E.; Cass, A. E. G.; O'Regan, B.; Durrant, J. R. *J. Electroanal. Chem.* **2001**, *517*, 20.
(2) Topoglidis, E.; Cass, A. E. G.; Gilardi, G.; Sadeghi, S.; Beaumont, N.; Durrant, J. R. *Anal. Chem.* **1998**, *70*, 5111.
(3) Topoglidis, E.; Campbell, C. J.; Cass, A. E. G.; Durrant, J. R. *Langmuir* **2001**, *17*, 7899.
(4) Huang, I. Y.; Lee, M. C. *Sens. Actuators, B* **2008**, *132*, 340.
(5) Zhang, F.; Wang, X.; Ai, S.; Sun, Z.; Wan, Q.; Zhu, Z.; Xian, Y.; Jin, L.; Yamamoto, K. *Anal. Chim. Acta* **2004**, *519*, 155.
(6) Wang, J. X.; Sun, X. W.; Wei, A.; Lei, Y.; Cai, X. P.; Li, C. M.; Dong, Z. L. *Appl. Phys. Lett.* **2006**, *88*, 233106.
(7) Wei, A.; Sun, X. W.; Wang, J. X.; Lei, Y.; Cai, X. P.; Li, C. M.; Dong, Z. L.; Huang, W. *Appl. Phys. Lett.* **2006**, *89*, 123902.
(8) Chen, L. Y.; Gu, B. X.; Zhu, G. P.; Wu, Y. F.; Liu, S. Q.; Xu, C. X. *NANO* **2007**, *2*, 281.
(9) Yaropolov, A. I.; Tarasevich, M. R.; Varfolomeev, S. D. *Bioelectrochem. Bioenerg.* **1978**, *5*, 18.
(10) Liu, S. Q.; Chen, A. C. *Langmuir* **2005**, *21*, 8409.
(11) Jia, J. B.; Wang, B. Q.; Wu, A. G.; Cheng, G. J.; Li, Z.; Dong, S. J. *Anal. Chem.* **2002**, *74*, 2217.
(12) Lu, H. Y.; James, F. R.; Hu, N. F. *J. Phys. Chem. B* **2007**, *111*, 14378.
(13) Zhang, Y. C.; Heller, A. *Anal. Chem.* **2005**, *77*, 7758.
(14) Wellinder, K. G. *Eur. J. Biochem.* **1979**, *96*, 483.
(15) Vayssieres, L. *Adv. Mater.* **2003**, *15*, 464.
(16) Yao, K. X.; Sinclair, R.; Zeng, H. C. *J. Phys. Chem. C* **2007**, *111*, 2032.
(17) Gu, B. X.; Xu, C. X.; Zhu, G. P.; Liu, S. Q.; Chen, L. Y.; Li, X. S. *J. Phys. Chem. B* **2009**, *113*, 377.
(18) Luo, X. L.; Xu, J. J.; Zhang, Q.; Yang, G. J.; Chen, H. Y. *Biosens. Bioelectron.* **2005**, *21*, 190.
(19) Huang, R.; Hu, N. F. *Bioelectrochemistry* **2001**, *54*, 75.
(20) Xu, Q.; Mao, C.; Liu, N. N.; Zhu, J. J.; Sheng, J. *Biosens. Bioelectron.* **2006**, *22*, 768.
(21) Anderson, J. L.; Bowden, E. F.; Pickup, P. G. *Anal. Chem.* **1996**, *68*, R379.
(22) Heller, A. *Acc. Chem. Res.* **1990**, *23*, 128.
(23) Zhang, Y.; He, P. L.; Hu, N. F. *Electrochim. Acta* **2004**, *49*, 1981.
(24) Ruzgas, T.; Gorton, L.; Emneus, J.; Marko-Varga, G. *J. Electroanal. Chem.* **1995**, *391*, 41.
(25) Zhao, Y. D.; Zhang, W. D.; Chen, H.; Luo, Q. M.; Li, F. Y. *Sens. Actuators, B* **2002**, *87*, 168.
(26) Claude, P.; Andrieux, B. L.; Saveant, J. M.; Dounia, Y. *Langmuir* **2006**, *22*, 10807.
(27) Laviron, E. *J. Electroanal. Chem.* **1979**, *101*, 19.
(28) Andreu, R.; Ferapontova, E. E.; Gorton, L.; Calvente, J. J. *J. Phys. Chem. B* **2007**, *111*, 469.
(29) Chen, X.; Ruan, C.; Kong, J.; Deng, J. *Anal. Chim. Acta* **2000**, *412*, 89.
(30) Xiang, C. L.; Zou, Y. J.; Sun, L. X.; Xu, F. *Anal. Lett.* **2008**, *41*, 2224.
(31) Kamin, R. A.; Wilson, G. S. *Anal. Chem.* **1980**, *52*, 1198.

JP900048M